Submitted, accepted and published by:
Fuel Processing Technology137 (2015) 24-30

Syngas/H_2 production from bioethanol in a continuous Chemical-Looping Reforming prototype

F. García-Labiano*[a], E. García-Díez[a], L. F. de Diego[a], A. Serrano[a], A. Abad[a], P. Gayán[a], J. Adánez[a], J. A.C. Ruíz[b]

[a] Department of Energy and Environment, Instituto de Carboquímica (ICB-CSIC), Miguel Luesma Castán 4, 50018 Zaragoza, Spain.

[b] Centro de Tecnologias do Gás e Energias Renováveis (CTGAS-ER), Av. Capitão Mor Gouveia, Natal, Brazil

* Corresponding author: Tel.: +34 976 733 977; fax: +34 976 733 318,

E-mail address: glabiano@icb.csic.es (F. García-Labiano)

Instituto de Carboquímica (ICB-CSIC), Miguel Luesma Castán 4, 50018 Zaragoza, Spain.

Abstract:

Chemical-looping reforming (CLR) allows H_2 production without CO_2 emissions into the atmosphere. The use of a renewable fuel, bioethanol, in an auto-thermal CLR process has the advantage to produce H_2 with negative CO_2 emissions. This work presents the experimental results obtained in a continuously operating CLR unit (1 kW_{th}) using ethanol as fuel. Two NiO-based oxygen carriers were used during more than 50 hours of operation. The influence of variables such as temperature, water-to-fuel

and oxygen-to-fuel molar ratios was analysed. Full conversion of ethanol was accomplished and carbon formation was easily avoided. A syngas composed by ≈61 vol.% H_2, ≈32 vol.% CO, ≈5 vol.% CO_2 and ≈2 vol.% CH_4 was reached at auto-thermal conditions for both materials. Gas composition was closed to the given by the thermodynamic equilibrium. These results demonstrate the technical viability of H_2/syngas production by using bioethanol in an auto-thermal CLR process.

Keywords: hydrogen; chemical-looping reforming; bioethanol, CO_2 emissions.

1. **Introduction:**

The concentration of carbon dioxide in the atmosphere is increasing continuously due to the use of anthropogenic sources [1]. Very recently, the world's most important CO_2 monitoring station at Mauna Loa recorded short term CO_2 concentrations above 400 parts per million, the highest levels found on earth in millions of years. Therefore, new solutions are urgently needed to enforce CO_2 emissions reduction.

CO_2 emissions from human activity arise from a number of different sources, mainly from the combustion of fossil fuels. Carbon capture and storage (CCS) has been identified as an essential technology to meet the internationally agreed goal of limiting the temperature increase to 2 ºC [2, 3]. This option is mainly fitted in the scenario of large power plants or industrial processes. However, diffuse emissions derived from transport represent an important part (≈21%) of the global CO_2 emissions [4]. The use of hydrogen has been considered during last years as a promising option to reduce CO_2 emissions from mobile sources [5]). However,

hydrogen is an energetic vector that needs to be obtained from primary energy sources. Hydrogen production by most existing technologies entails substantial use of fossil fuels and CO_2 emissions. In fact, steam methane reforming is currently the most common and developed technology used for hydrogen production at large scales, and it is likely to remain in the nearby future. Partial oxidation is the most appropriate technology to produce H_2 from heavier feed-stocks such as heavy oil residues and coal [6]. In a low-carbon context, two possibilities arise: the use of carbon-free renewable energy sources [7] or the integration of fossil-fuel H_2 production and CO_2 capture processes [6]. The high cost associated to both solutions can be considered as the main barrier to further development.

During last years, innovative technologies for CO_2 capture have arisen. Among them, chemical looping is considered as the highest technology regarding cost reduction benefit among all available options although the time to commercialization is expected to be large [8, 9].

Chemical looping processes have got a great development during last decade [10], including both Chemical-Looping Combustion (CLC) for heat/electricity production and Chemical looping Reforming (CLR) for syngas/H_2 production. These processes are based on the transfer of oxygen from air to the fuel by means of a solid oxygen carrier avoiding direct contact between fuel and air. In the CLR process the air to fuel ratio is kept low to prevent the complete oxidation of the fuel to CO_2 and H_2O. Fig. 1 shows the scheme of a typical CLR process. A N_2 free gas stream concentrated in H_2 and CO is obtained at the outlet of the fuel reactor. Moreover, the Air Separation Unit (ASU) required in the conventional auto-thermal reforming for CO_2 capture is here avoided. In addition, higher H_2 yield is obtained

when a Water-Gas Shift (WGS) reactor is used downstream the CLR system, but with the advantage that the CO_2 capture is accomplished in the global process and no additional energy from an external source is needed [11].

Most of the technology development up to now has been carried out using CH_4 as fuel. The CLR process has been demonstrated at atmospheric pressure in continuous units [12, 13], at laboratory scale [14] and in a 140 kWth pilot plant [15]. In addition, the effect of pressure in a semi-continuous fluidized bed reactor has been also analysed [16]. All the above works were carried out using Ni-based oxygen carriers and gaseous fuels. Very recently, a liquid fuel, sulfur-free kerosene, has been used for the first time for H_2 production via CLR in a 300 Wth unit [17].

The above technologies are all based in the use of fossil fuels. However, interesting options are open if the fuel comes from renewable sources (biomass or biofuels) [18, 19] since negative CO_2 emissions can be achieved [20, 21]. This result especially interesting considering the CO_2 price in the future carbon markets. Although carbon price have fallen to low levels during recent years, reaching values as low as $3/tonne in April 2013, most of the future scenarios assume a continuous rising in the price of CO_2. In the new policies scenario reported by the IEA [2], the price will increases up to ≈$20/tonne in 2020 and ≈$40/tonne in 2035. This price is even higher in the 450 scenario, reaching values of $20-$35/tonne in 2020, $95/tonne in 2030 and $125 in 2035.

Currently, liquid fuels from renewable energies are becoming more relevant. Among them, ethanol (EtOH) offers high possibilities due to the large amount available. Currently, USA and Brazil are the main ethanol producers worldwide with more than 28440 and 15783 thousand tonnes in 2013 [22], respectively.

Furthermore, the ethanol production estimated for 2014 was around 90 billion litres, which involves a decrease in the greenhouse gas emissions of 291 thousand tonnes per day [23].

Recently, Cormos, [24] has evaluated the hydrogen production from bioethanol at industrial scale (300 MW_{th}) with different carbon capture options. He concluded that chemical looping design showed promising energy efficiency and total carbon capture. Very recently, experimental results of CLR process of ethanol were obtained in a packed bed reactor [25]. However, no experimental data regarding this process have been carried out up to now in a continuous unit.

The objective of this work is to demonstrate the technical feasibility of syngas/H_2 production in a 1 kW_{th} continuous unit by integrating a low cost technology including inherent CO_2 capture, CLR, and the most popular biofuel, ethanol. The effect of the main operating conditions such as oxygen-to-fuel molar ratio, temperature, and H_2O/EtOH molar ratio is evaluated.

2. Experimental

2.1 Materials

Ni-based materials were the first materials used for demonstrating the viability of chemical looping as a carbon capture technology. Moreover, the catalytic activity of metallic Ni made of them suitable materials for H_2 production when reforming processes are involved. An additional advantage of the joint use of these Ni-based materials and bioethanol is the absence of deactivation processes by sulphur that normally happens when fossil fuels are used [26].

Two different oxygen carriers (OC) based on NiO have been used in this work. The materials have been designated with the metal oxide followed by its weight content

and the inert used as support. The NiO21-γAl_2O_3 was obtained by the incipient wetness impregnation method using commercial γ-Al_2O_3 (Puralox NWa-155, Sasol Germany GmbH) as support [27]. The NiO18-αAl_2O_3 was prepared by hot incipient wet impregnation [28], a modification of the method above mentioned, to increase the amount of NiO which could be introduced into the support in each impregnation stage.

These oxygen carriers have been patented by CSIC [29, 30]. The reduction and oxidation kinetics of these oxygen carriers with regards to the main gaseous products existing in CLC and CLR processes, and their catalytic activity have been determined in previous works [31, 32]. Table 1 shows the physical characteristics of both oxygen-carriers and the two inert used as support. After operation in plant, nickel was present as NiO and $NiAl_2O_4$ in both materials although the NiO/$NiAl_2O_4$ ratio was different for each oxygen carrier. It must be considered that both nickel compounds are active for oxygen transfer although with very different reactivities. The lower reactivity of the NiO21-γAl_2O_3 oxygen carrier was due to the higher interaction between the NiO and the γ-Al_2O_3 to form $NiAl_2O_4$. On the contrary, this interaction was reduced when using the α-Al_2O_3 as support.

Ethanol, 96 vol.%, was used as fuel. The simulation of bioethanol with different water contents was accomplished by addition of different amounts of water to the fuel.

2.2 1 kW_{th} experimental facility (ICB-CSIC-liq1)

Fig. 2 shows a schematic diagram of the 1 kW_{th} Chemical Looping unit, designated as ICB-CSIC-liq1, used in this work. The unit was composed of two interconnected

fluidized-bed reactors, a system for gas and liquid feeding, and a system for gas analysis.

The fuel reactor, FR, (1) consisted of a bubbling fluidized bed in which NiO is reduced to Ni, and the fuel is mainly oxidised to CO and H_2. This FR had a conical shape (0.08 m top i.d. and 0.026 m bottom i.d.) and a bed height of 0.15 m. This shape avoided solids elutriation as a consequence of the increase in the gas velocity by the gas generated during ethanol processing. Reduced oxygen carrier particles overflowed into the air reactor, AR, (3) through a U-shaped fluidized bed loop seal (2) to avoid the mixing of the gases between FR and AR. The regeneration of the carrier took place at the AR, which consisted of a bubbling fluidized bed (0.052 m i.d.) with a bed height of 0.15 m, followed by a riser (4) (1.8 m height and 0.026 m i.d.). Secondary air can be injected at the top of the dense bed to help the particles transport through the riser. The oxygen-carrier, recovered by the cyclone (5), was sent to a solids reservoir, setting the particles ready to another cycle, and avoiding the gas leakage between the riser and the FR. A diverting solid valve (6) located just below the cyclone allowed the measurement of the solid circulating rate. The oxygen carrier returned to the FR by gravity from the solids reservoir through a solid control system (7). The fine particles produced by attrition were recovered by the filters (8) located downstream the FR and AR.

The gases were fed by means of specific mass-flow controllers. The ethanol and water were injected to a heater (10) using two peristaltic pumps (9). The liquids were evaporated and then fed into the FR mixed with N_2.

The gas outlet streams of the FR and AR were drawn to respective on-line gas analysers to get continuous data of gas composition. The outlet gas from the FR was

normally composed by N_2, CO_2, H_2O, CH_4, H_2, and CO. Pure N_2 or depleted air was obtained at the AR outlet. The possible carbon formation on the FR would be detected as CO_2 at the AR outlet.

CH_4, CO, CO_2 were measured via a non-dispersive infrared analyser (Siemens/Ultramat 23), H_2 using a thermal conductivity analyser (Maihak S710), and the O_2 by a paramagnetic analyser (Siemens/Oxymat 5E). A Gas Chromatograph (Clarus 580 with Model Arnel 4016 PPC and Haye Sep columns) was also established on line to detect the possible hydrocarbon compounds coming from ethanol decomposition or reaction.

2.3 Operational conditions

Test under different operational conditions were carried out in the 1 kW_{th} unit using ethanol as fuel. The solids inventory in the system was ≈1.3 kg and ≈1.8 kg for NiO21-γAl_2O_3 and NiO18-αAl_2O_3, respectively.

The total air flow in the AR was 1100 Nl/h, divided between primary (700 Nl/h) and secondary (400 Nl/h) air. The total gas inlet flow in the FR was 150 Nl/h. The flow of EtOH injected were ≈100 g/h which corresponds to ≈675 Wth.

Tests to evaluate the effect of the main operating conditions such as temperature (850-950 ºC), water to ethanol molar ratio (0-1), and oxygen to ethanol molar ratio (0.6-6) were carried out.

The steady-state for the different operating conditions was maintained at least for forty five minutes in each test. This gives a total of about 80 hours at high temperature, from which 50 hours corresponds to ethanol-fuelled operation with both oxygen carriers. Agglomeration problems were never detected during operation and both materials showed good hydrodynamic behaviour. Furthermore,

the attrition rate was low for both oxygen carriers reaching values of ≈0.04 wt%/h and ≈0.01 wt%/h for the NiO21-γAl_2O_3 and NiO18-αAl_2O_3, respectively.

2.4 Main reactions

CO_2, CO, CH_4, and H_2 (and N_2) were the main gaseous products found at the outlet of the FR, and N_2, O_2, (and CO_2 if carbon formation in FR takes place) at the outlet of the AR. The main reactions happening inside both reactors are given below.

In the fuel reactor takes place the direct oxidation of the ethanol with the NiO, or some other intermediate gaseous compounds, to give CO_2 and H_2O as final products (R1-R4). These reactions are all exothermic and are necessary to give the heat necessary to produce the endothermic reforming reactions in an auto-thermal process. Syngas/H_2 can be produced via partial oxidation (R5) or via steam fuel reforming (R6-R8). Fatsikostas et al. [33] determined the main products obtained from ethanol decomposition in an empty reactor or in presence of alumina and nickel. According to these authors, ethanol can suffer carbon break change to produce lighter hydrocarbons (R9, R11-R12) and carbon (R10, R13). The ethanol decomposition routes can change depending on the operational conditions existing in the reactor. This carbon can be gasified inside the reactor in presence of H_2O or CO_2 (R14-R15). The water gas shift reaction is always present in the gaseous phase (R16).

The main reaction taking place in the air reactor is the Ni oxidation to give NiO (R.17). The carbon formed in the fuel reactor can be also burnt to give CO_2 (R18).

Inside the Fuel reactor:

Oxidation

$C_2H_5OH + 6\ NiO \rightarrow 6\ Ni + 2\ CO_2 + 3\ H_2O$ (R.1)

$CH_4 + 4\ NiO \rightarrow 4\ Ni + CO_2 + 2\ H_2O$ (R.2)

$H_2 + NiO \rightarrow Ni + H_2O$ (R.3)

$CO + NiO \rightarrow Ni + CO_2$ (R.4)

Partial oxidation

$C_2H_5OH + NiO \rightarrow Ni + 2\ CO + 3\ H_2$ (R.5)

Steam reforming catalysed by Ni

$C_2H_5OH + H_2O \rightarrow 2\ CO + 4\ H_2$ (R.6)

$C_2H_5OH + 3\ H_2O \rightarrow 2\ CO_2 + 6\ H_2$ (R.7)

$CH_4 + H_2O \rightarrow CO + 3\ H_2$ (R.8)

Carbon chain breakage

$C_2H_5OH \leftrightarrow C_2H_4 + H_2O$ (R.9)

$C_2H_4 \leftrightarrow 2\ C + 2\ H_2$ (R.10)

$C_2H_5OH \leftrightarrow C_2H_4O + H_2$ (R.11)

$C_2H_4O \leftrightarrow CH_4 + CO$ (R.12)

$CH_4 \leftrightarrow C + 2\ H_2$ (R.13)

Carbon gasification

$C + H_2O \rightarrow CO + H_2$ (R.14)

$C + CO_2 \rightarrow 2\ CO$ (R.15)

Water-gas shift

$CO + H_2O \leftrightarrow CO_2 + H_2$ (R.16)

Inside the Air Reactor:

$Ni + ½\ O_2 \rightarrow NiO$ (R.17)

Carbon combustion

$$C + O_2 \rightarrow CO_2 \quad \text{(R.18)}$$

2.5 Mass balance

A mass balance regarding the oxygen involved in the process of oxygen carrier reduction for syngas production and oxidation for regeneration has been carried out. The mass balance in the FR of the CLR system, based on the oxygen to EtOH molar ratio, O_{NiO}/EtOH, can be expressed as

$$\frac{F_s x_{NiO,AR}}{M_{NiO}} \Delta X_s = F_{EtOH} \left({}^{O_{NiO}}/_{EtOH} \right) \quad (1)$$

where F_s is the oxygen carrier circulation flow-rate, $x_{NiO,AR}$ is the fraction of NiO present in the oxygen carrier at the outlet of the AR, M_{NiO} is the molecular weight of NiO, and F_{EtOH} is the molar flow of EtOH fed to the FR. The O_{NiO}/EtOH molar ratio is the amount of oxygen transferred by chemical reaction with NiO to the fuel per mol of ethanol fed. The variation of the oxygen carrier conversion between the fuel and air reactors, ΔX_s, was defined as:

$$\Delta X_s = X_{AR} - X_{FR} \quad (2)$$

$$X_{AR} = \frac{x_{NiO,AR} - x_{NiO,red}}{x_{NiO,ox} - x_{NiO,red}} \quad (3)$$

$$X_{FR} = \frac{x_{NiO,FR} - x_{NiO,red}}{x_{NiO,ox} - x_{NiO,red}} \quad (4)$$

being X_{AR} and X_{FR} the conversion of the oxygen carrier at the exit of the AR and FR respectively, $x_{NiO,AR}$ and $x_{NiO,FR}$ the fraction of NiO in the oxygen carrier at the exit of the AR and FR respectively, and $x_{NiO,ox}$ and $x_{NiO,red}$ the fraction of NiO when the oxygen carrier is fully oxidized or reduced respectively.

The mass balance in the AR based on the reacted oxygen can be written as:

$$\frac{F_s x_{NiO,AR}}{M_{NiO}} \Delta X_s = F_{O2,in} \Delta X_{O2} \quad (5)$$

$$\Delta X_{O2} = \frac{F_{O2,in} - F_{O2,out} - F_{CO2}}{F_{O2,in}} \quad (6)$$

where $F_{O2,in}$ and $F_{O2,out}$ are the molar flow of oxygen fed to or leaving the AR, and ΔX_{O2} is the conversion of the oxygen in the AR which is consumed by the oxygen carrier. F_{CO2} corresponds to the CO_2 detected at the AR as a consequence of the combustion of the carbon formed in the FR.

2.6 Control of the oxygen used in the system

In a chemical looping process it is very important to control the oxygen available for reaction in the FR. The solids circulation rate between reactors must be high enough to transfer the oxygen necessary for the desired reactions. This will depend on the oxygen transport capacity of the oxygen carrier which is a function of the metal oxide content and of the oxygen transfer in the redox reactions [34].

In CLC, the control of the oxygen fed into the fuel reactor is normally carried out by controlling the solids circulation rate in the system. Some excess of oxygen over the stoichiometry is necessary to reach high combustion efficiencies. In this specific case, more than 6 moles of NiO must be fed into the FR per mole of ethanol to obtain CO_2 and H_2O as final products (see R1).

In CLR, where under stoichiometric oxygen ratios must be used, an alternative method is recommended. The control of the oxygen to ethanol molar ratio can be accomplished by limiting the oxygen supplied by the air flow fed to the AR. In the ICB-CSIC-liq1 unit this was carried out by diluting this stream with N_2. This method has important consequences from an industrial point of view because it allows an easy operation, an accurate oxygen flow control from the AR to the FR, and, in addition, pure N_2 can be obtained at the outlet of the AR [11, 15]. In this

case, all oxygen entering the AR is transferred to the FR (i.e. ΔXO_2=1) and the global air to EtOH ratio is equal to the O_{NiO}/EtOH molar ratio used for syngas production in the FR. Obviously, this is true when carbon formation in FR is zero (F_{CO2}=0).

3. Results and discussion

3.1 Effect of the fuel reactor temperature

The effect of the fuel reactor temperature on syngas production was tested in the range of 850 to 950 ºC. The other operating variables (ethanol feeding, H_2O/EtOH, and O_{NiO}/EtOH molar ratios) were kept constant. As an example, Fig. 3 shows the syngas production composition expressed per mol of EtOH at the three temperatures evaluated with the NiO21-γAl_2O_3 oxygen carrier.

Ethanol conversion was complete at all temperatures, with a small concentration of methane detected. That means that CH_4 is an important intermediate product in the whole reaction system, which is produced by chain breakage in carbonaceous fuels (R.11-R.12). In any case, it was observed that the FR temperature hardly affected the gas composition.

3.2 Effect of the water to fuel molar ratio

In a CLR global process, water addition is necessary because increases H_2 production and avoids carbon formation. H_2O can be directly fed to the FR, to the water gas shift reactor or to both places. However, it must be considered that renewable ethanol usually contains a certain amount of water due to the production method or improper storage. The production of ethanol as a fuel can be divided into two purities: anhydrous, with a water content less than 1 wt.%, and hydrous with a water content between 5 and 10 wt.%. Since H_2O addition in a CLR process is

needed, direct application of hydrous ethanol would be advantageous because will reduce energy costs during the production stage [35].

In this work, three different H_2O/EtOH molar ratios were evaluated (0, 0.5 and 1) for the same ethanol feeding and maintaining constant the inlet stream to the FR at 150 Nl/h. Fig. 4 shows the effect of the H_2O/EtOH molar ratio on the gas product concentration at the exit of the FR for the NiO21-γAl_2O_3 oxygen carrier.

An increase in the amount of the water injected produced a slight increase on the H_2 and CO_2 concentrations and a decrease on the CO and CH_4 concentrations. This variation was produced by the water enhancement of the steam reforming reactions catalysed by Ni, including both ethanol and CH_4 (R.6-R.8), and especially by the water gas shift reaction (R.16). A proof of this is that the amount of syngas ($CO+H_2$) produced remains almost constant at all molar ratios. This behaviour was similar to a previous work using methane as fuel [14].

Finally, it should be remarked that the effect observed was similar for both oxygen carriers, and that no carbon formation was observed in any case at these operating conditions.

3.3 Effect of the oxygen to fuel molar ratio

The main parameter in a CLR process is the oxygen to fuel molar ratio used in the FR for syngas production. As above explained, the method used in this work to control the amount of oxygen transported by the oxygen carrier as NiO to the FR was the control of the oxidation reaction in the AR by limiting the oxygen feeding. The oxygen concentration in the AR inlet stream was varied from 2 to 21 vol.% by diluting the air with N_2 in order to maintain constant the total gas flow and the hydrodynamic properties in the system. These values correspond to O_{NiO}/EtOH

ratios from 0.6 to 6. In all cases, the solid circulation rate was maintained constant at 9 kg/h.

Fig. 5 shows the effect of the O_{NiO}/EtOH molar ratio on the syngas composition obtained in the FR outlet stream with different H_2O/EtOH molar ratios for the two oxygen carriers, NiO21-γAl_2O_3 and NiO18-αAl_2O_3.

A complete conversion of ethanol was achieved in all cases. Values of O_{NiO}/EtOH above 6 represented combustion conditions and the gas was mainly composed by CO_2 and H_2O. For the specific case of Ni-based oxygen carriers, some CO and H_2 appeared always at equilibrium [10]. A decrease in the O_{NiO}/EtOH molar ratio produced an increase in the H_2, CO, and CH_4 concentrations and a decrease in the CO_2 (and H_2O) concentration. This was due to the contribution of the different reactions aforementioned (R.1-R.16) to the overall global process. In this sense, partial oxidation and reforming reactions are being more relevant in comparison to oxidation as the O_{NiO}/EtOH used is lower.

To maximize syngas production without H_2O feeding, O_{NiO}/EtOH molar ratios about 1 should be used. Values lower to 1 means that no enough oxygen (in the form of NiO) is contributed by the oxygen carrier to produce syngas, (even for the lower oxidation stoichiometry as it is the partial oxidation, R.5). In such case, carbon should be formed through reactions R.10 or R.13. In fact, data obtained in Fig. 5b at O_{NiO}/EtOH≈0.6 showed a high amount of H_2 but some CO_2 was detected at the outlet of the AR as a consequence of the combustion of the carbon formed in the FR. Obviously, an increase in the H_2O content produced a decrease in carbon formation through gasification reaction (R.14). In any case it is worthy to note that

these operating conditions will never be used in a real case where auto-thermal conditions must be reached.

In an autothermal-CLR process, the heat necessary for the endothermic reduction reactions (R.6-R.8) is given by the hot solids coming from the AR and also by the partial exothermic reactions in the FR (R.1-R5). A calculation showed that a molar ratio O_{NiO}/EtOH range between 1.2 and 1.5, depending on the water to fuel molar ratio used, was necessary to reach auto-thermal conditions. A dry syngas composed by ≈59-62 vol.% H_2, ≈36-27 vol.% CO, ≈1-10 vol.% CO_2, and ≈1-3 vol.% CH_4 was experimentally obtained in the CLR unit using ethanol as fuel for both oxygen carriers at these operating conditions. The syngas composition was quite similar in comparison to that obtained using CH_4 as fuel [9]. If we consider that the syngas produced is further associated with a WGS and a H_2/CO_2 separation unit, a final amount of ≈4.8 moles of H_2 could be finally obtained per mol of ethanol fed. This can be considered a good result given that the maximum theoretical value based only in a mass balance is 5 mol H_2/mol EtOH.

The thermodynamic equilibrium gas compositions were also represented in Fig. 5 by continuous lines. The equilibrium data were obtained with the HSC Chemistry 6.1 software [36] which uses the method of minimization of the Gibbs free energy in the system. As mentioned earlier, an increase in the H_2O/EtOH molar ratio produced an increase in the H_2 and CO_2 and a decrease in the CO concentrations, both in the experimental and in the equilibrium data. It was observed that syngas compositions experimentally obtained for both oxygen carriers were very close to that given by the thermodynamic equilibrium.

3.4 Effect of the solids circulation rate, F_s

An important feature of the CLR process herein used is the possibility to control the oxygen used for syngas production in the FR by limiting the oxygen supplied by the air flow fed to the AR, i.e. controlling ΔX_{O2} in eq. (6). However, for an oxygen carrier with a given NiO content, the same oxygen reacted, ΔX_{O2} (and therefore the same syngas composition) can be accomplished using different combinations of solid circulation rates, F_s, and solid conversions, ΔX_s (see eq. 5).

To better analyse this behaviour, oxidation conversion of the oxygen carriers, X_{FR} and X_{AR}, at the exit of the FR and AR were determined in a thermobalance with samples extracted from the unit after the tests. Obviously, ΔX_s values can be further calculated by means of eq. (2), which have a direct dependency with O_{NiO}/EtOH molar ratios.

As an example, Fig. 6a shows the solid conversions, X_{AR} and X_{FR}, of the Ni21-γAl_2O_3 oxygen carrier as a function of the O_{NiO}/EtOH molar ratio for different solid circulation rates, F_s. The solid conversion at the exit of the AR, X_{AR}, was very similar in all cases independently on the solid circulation rate. It is also remarkable that the oxygen carrier returned to the FR incompletely oxidised at typical CLR operating conditions. That means that the oxygen carrier contains NiO and $NiAl_2O_4$, which transfer oxygen for syngas production, and metallic Ni that can act as catalyst in the reforming reactions (R.6-R.8). On the contrary, the conversion at the exit of the FR, X_{FR}, was very dependent on the solid circulation rate, as it is shown in Fig. 6a. Samples fully reduced were only obtained for the lowest solid circulation rate, F_s=3 kg/h, and O_{NiO}/EtOH molar ratios above 3, although this situation will never be used in a CLR process. Considering the auto-thermal conditions

previously determined, the solid conversions varied between ≈0.4 and ≈0.6, for an oxygen carrier with a 21 wt.% NiO.

Finally, a comparison between the two oxygen carriers was done for the same solid circulation rate (F_s=9 kg/h), i.e. residence time in the fuel reactor. Even though a similar behaviour was observed for both oxygen carriers, the solid conversions, X_{AR} and X_{FR}, obtained with the NiO18-αAl_2O_3 were lower. The higher presence of free NiO in the oxygen carrier NiO18-αAl_2O_3, which is more reactive than the $NiAl_2O_4$, implies a lower solid conversion at the outlet of the FR, X_{FR}. As mentioned earlier, the control of the oxygen to ethanol molar ratio was accomplished by limiting the oxygen reacted with the oxygen carrier in the AR. That means that, for a given ratio, the same amount of oxygen was transferred from the carrier to the fuel, i.e. the same ΔX_s, independently of the material used. Therefore, the solid conversion reached in the AR, X_{AR}, was also lower for the NiO18-αAl_2O_3 oxygen carrier.

In any case, both materials are suitable for syngas production in an auto-thermal CLR process using bioethanol as fuel.

4. Conclusions

The continuous Chemical-Looping Reforming of ethanol has been evaluated during more than 50 hours using two different NiO-based materials. Both oxygen carriers exhibited a good performance during the whole experimentation. The gas concentrations obtained in the syngas were very close to the values given by the thermodynamic equilibrium and pure N_2 was obtained in the air reactor.

Furthermore, ethanol conversion was complete at all operating conditions and carbon formation was easily avoided. This work has demonstrated the possibility of

integrating a low cost technology for H_2 production with inherent CO_2 capture, the CLR, and the most popular biofuel. In addition, the renewable character of the biofuel makes interesting the process considering that negative CO_2 emissions could be achieved in some cases.

Acknowledgements

This work partially supported by the Spanish Ministry for Science and Innovation (MICINN project ENE2011-26354) and FEDER, and by CTGAS-ER (project OTT20130989). A. Serrano also thanks the Spanish Ministry of Economy and Competitiveness for the F.P.I fellowship.

References

[1] T.F. Stocker, D. Qin, G.K. Plattner, M. Tignor, Allen, S.K. Allen, Boschung, J. Boschung, A. Nauels, Y. Xia, V. Bex, P.M. Midgley, IPCC, 2013: Climate Change 2013: The Physical Science Basis. Contribution of Working Group I to the Fifth Assessment Report of the Intergovernmental Panel on Climate Change. Cambridge University Press, Cambridge and New York 2013.

[2] International Energy Agency (IEA). World Energy Outlook 2013.

[3] Global CCS Institute, The Global Status of CCS: 2014, Melbourne, Australia, 2014.

[4] International Energy Agency (IEA). CO_2 emissions from fuel combustion - highlights. 2013 Edition.

[5] A. Kontogianni, C. Tourkolias, E.I. Papageorgiou, Revealing market adaptation to a low carbon transport economy: Tales of hydrogen futures as perceived by fuzzy cognitive mapping, Int. J. Hydrogen Energy. 38 (2013) 709-722.

[6] K. Damen, M. van Troost, A. Faaij, W. Turkenburg, A comparison of electricity and hydrogen production systems with CO_2 capture and storage. Part A: Review and selection of promising conversion and capture technologies, Prog. Energy Combust. Sci. 32 (2006) 215-246.

[7] T. Abbasi, T.S. Abbasi, 'Renewable' hydrogen: Prospects and challenges, Renew. Sustainable Energy Rev. 15 (2011) 3034-3040.

[8] M. Zhao, A.I. Minett, T. Harris, A review of techno-economic models for the retrofitting of conventional pulverised-coal power plants for post-combustion capture (PCC) of CO_2, Energy Environ. Sci. 6 (2013) 25-40.

[9] L-S. Fan, L. Zeng, W. Wang, S. Luo, Chemical looping processes for CO_2 capture and carbonaceous fuel conversion - Prospect and opportunity, Energy Environ. Sci. 5 (2012) 7254-7280.

[10] J. Adánez, A. Abad, F. García-Labiano, P. Gayán, L.F. de Diego, Progress in chemical-looping combustion and reforming technologies, Prog. Energy Combust. Sci. 38 (2012) 215-282.

[11] M. Ortiz, A. Abad, L.F. de Diego, F. García-Labiano, P. Gayán, J. Adánez, Optimization of hydrogen production by Chemical-looping auto-thermal reforming working with Ni-based oxygen-carriers, Int. J. Hydrogen Energy. 36 (2011) 9663-9672.

[12] M. Rydén, A. Lyngfelt, T. Mattisson, Synthesis gas generation by chemical-looping reforming in a continuously operating laboratory reactor, Fuel. 85 (2006) 1631-1641.

[13] M. Rydén, A. Lyngfelt, T. Mattisson, Chemical-looping combustion and chemical-looping reforming in a circulating fluidized-bed reactor using Ni-based oxygen carriers, Energy Fuel. 22 (2008) 2585-2597.

[14] L.F. de Diego, M. Ortiz, F. García-Labiano, J. Adánez, A. Abad, P. Gayán, Hydrogen production by chemical-looping reforming in a circulating fluidized bed reactor using Ni-based oxygen carriers, J. Power Sources. 192 (2009) 27-34.

[15] T. Pröll, J. Bolhàrd-Nordenkampf, P. Kolbitsch, H. Hofbauer, Syngas and a separate nitrogen/argon stream via chemical looping reforming - A 140 kW pilot plant study, Fuel. 89 (2010) 1249-1256.

[16] M. Ortiz, L.F. de Diego, A. Abad, F. García-Labiano, P. Gayán, J. Adánez, Hydrogen production by auto-thermal chemical-looping reforming in a pressurized fluidized bed reactor using Ni-based oxygen carriers, Int. J. Hydrogen Energy. 35 (2010) 151-160.

[17] P. Moldenhauer, M. Rydén, T. Mattisson, A. Lyngfelt, Chemical-looping combustion and chemical-looping reforming of kerosene in a circulating fluidized-bed 300 W laboratory reactor, Int. J. Greenhouse Gas Control. 9 (2012) 1-9.

[18] Z. Huang, F. He, Y. Feng, K. Zhao, A. Zheng, S. Chang, H. Li, Synthesis gas production through biomass direct chemical looping conversion with natural hematite as an oxygen carrier, Bioresour. Technol. 140 (2013) 138-145.

[19] P. Pimenidou, G. Rickett, V. Dupont, M.V. Twigg, High purity H_2 by sorption-enhanced chemical looping reforming of waste cooking oil in a packed bed reactor, Bioresour. Technol. 101 (2010) 9279-9286.

[20] J.A. Mathews, Carbon-negative biofuels, Energy Policy. 36 (2008) 940-945.

[21] W. Budzianowski, Negative carbon intensity of renewable energy technologies involving biomass or carbon dioxide as inputs, Renew. and Sustain. Energy Rev. 16 (2012) 6507-6521.

[22] International Energy Agency (IEA), Biofuels for transport-An international Perspective, 2004.

[23] Global Renewable Fuels Alliance, http://globalrfa.org/ (15/12/2014)

[24] C-C. Cormos, Renewable hydrogen production concepts from bioethanol reforming with carbon capture, Int. J. Hydrogen Energy. 39 (2014) 5597-5606.

[25] R. Md Zin, A.B. Ross, J.M. Jones, V. Dupont, Hydrogen from ethanol reforming with aqueous fraction of pine pyrolysis oil with and without chemical looping, Bioresour. Technol. 176 (2015) 257-266.

[26] F. García-Labiano, L.F. de Diego, P. Gayán, J. Adánez, A. Abad, C. Dueso, Effect of fuel gas composition in chemical-looping combustion with ni-based oxygen carriers. 1. Fate of sulfur, Ind. Eng. Chem. Res. 48 (2009) 2499-2508.

[27] P. Gayán, L.F. de Diego, F. García-Labiano, J. Adánez, A. Abad, C. Dueso, Effect of support on reactivity and selectivity of Ni-based oxygen carriers for chemical-looping combustion, Fuel. 87 (2008) 2641-2650.

[28] P. Gayán, C. Dueso, A. Abad, J. Adánez, L.F. de Diego, F. García-Labiano, NiO/Al_2O_3 oxygen carriers for Chemical-looping combustion prepared by impregnation and deposition-precipitation methods, Fuel. 88 (2009) 1016-1023.

[29] J. Adánez, L.F. de Diego, F. García-Labiano, P. Gayán, A. Abad, CSIC Patent WO2009/022046. 2009.

[30] J. Adánez, L.F. de Diego, F. García-Labiano, P. Gayán, A. Abad, CSIC Patent WO2009/101233. 2009.

[31] C. Dueso, M. Ortiz, A. Abad, F. García-Labiano, L.F. de Diego, P. Gayán, J. Adánez, Reduction and oxidation kinetics of nickel-based oxygen-carriers for chemical-looping combustion and chemical-looping reforming, Chem. Eng. J. 188 (2012) 142-154.

[32] M. Ortiz, L.F. de Diego, A. Abad, F. García-Labiano, P. Gayán, J. Adánez, Catalytic activity of ni-based oxygen-carriers for steam methane reforming in chemical-looping processes, Energy Fuels. 26 (2012) 791-800.

[33] A.N. Fatsikostas, X.E. Verykios, Reaction network of steam reforming of ethanol over Ni-based catalysts, J. of Catalysis. 225 (2004) 439-452.

[34] A. Abad, J. Adánez, F. García-Labiano, L.F. de Diego, P. Gayán, J. Celaya, Mapping of the range of operational conditions for Cu-, Fe-, and Ni-based oxygen carriers in Chemical-looping combustion, Chem. Eng. Sci. 62 (2007) 533-549.

[35] R. Munsin, Y. Laoonual, S. Jugjai, Y. Imai, An experimental study on performance and emissions of a small SI engine generator set fuelled by hydrous ethanol with high water contents up to 40%, Fuel. 106 (2013) 586-592.

[36] HSC Chemistry 6.1. Pori, Finland: Oututec Res. Oy; 2008.

Figure Captions

Fig. 1. Chemical Looping Reforming Process

Fig. 2. Schematic diagram of the 1 kWth chemical-looping reforming unit (ICB-CSIC-liq1).

Fig. 3. Effect of the fuel reactor temperature on the syngas composition. OC= NiO21-γAl_2O_3, H_2O/EtOH=1, O_{NiO}/EtOH=1.2.

Fig. 4. Effect of the H_2O/EtOH molar ratio in the syngas composition. OC=NiO21-γAl_2O_3, T_{FR}= 900 ºC, O_{NiO}/EtOH=1.2.

Fig. 5. Syngas composition obtained as a function of the oxygen-to-fuel molar ratio. a) NiO21-γAl_2O_3 , b) NiO18-αAl_2O_3. T= 900 ºC. Lines represent thermodynamic equilibrium. (▫,___, H_2O/EtOH = 0), (▵,- - -, H_2O/EtOH = 0.5), (○,…., H_2O/EtOH = 1).

Fig. 6. Solid conversion at the exit of the fuel and air reactors for different solid circulation rates. a) OC= NiO21-γAl_2O_3, b) NiO21-γAl_2O_3 and NiO18-αAl_2O_3 with F_s=9 kg/h. T_{FR}= 900 ºC. (▫, Solid conversion in the AR), (▵ , Solid conversion in the FR).

Tables

Table 1

Physical properties of the supports and the fresh oxygen-carriers

Sample	γ-Al_2O_3	α-Al_2O_3	NiO21-γAl_2O_3	NiO18-αAl_2O_3
Particle size (mm)	0.1-0.3	0.1-0.3	0.1-0.3	0.1-0.3
Apparent density (kg/m^3)	1300	2000	1700	2500
Porosity (%)	55.4	47.3	50.7	42.5
Specific surface area BET (m^2/g)	155	14.6	83.4	7
Mechanical strength (N)	-	-	2.6	4.1
XRD phases	γ-Al_2O_3	α-Al_2O_3	γ-Al_2O_3, $NiAl_2O_4$	α-Al_2O_3, NiO, $NiAl_2O_4$

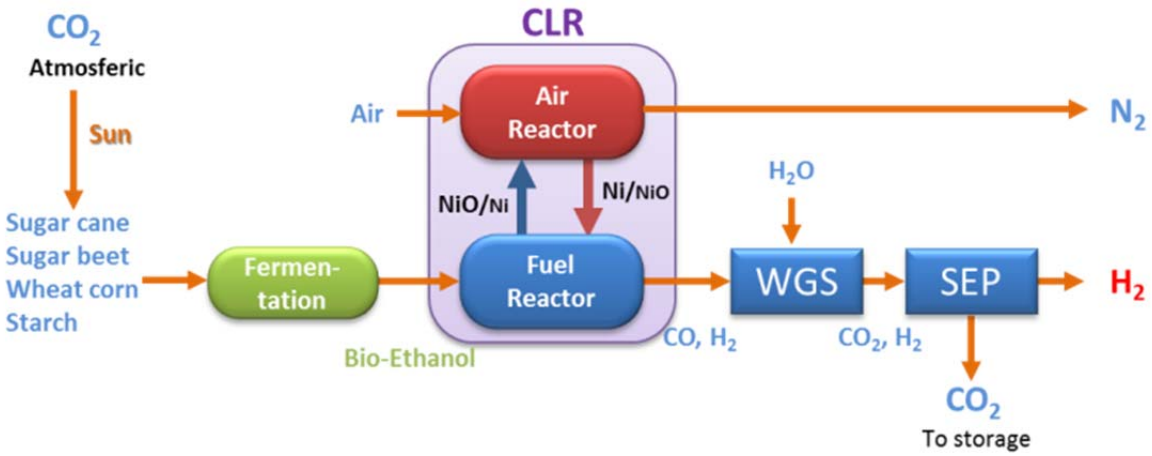

Fig. 1. Chemical Looping Reforming Process

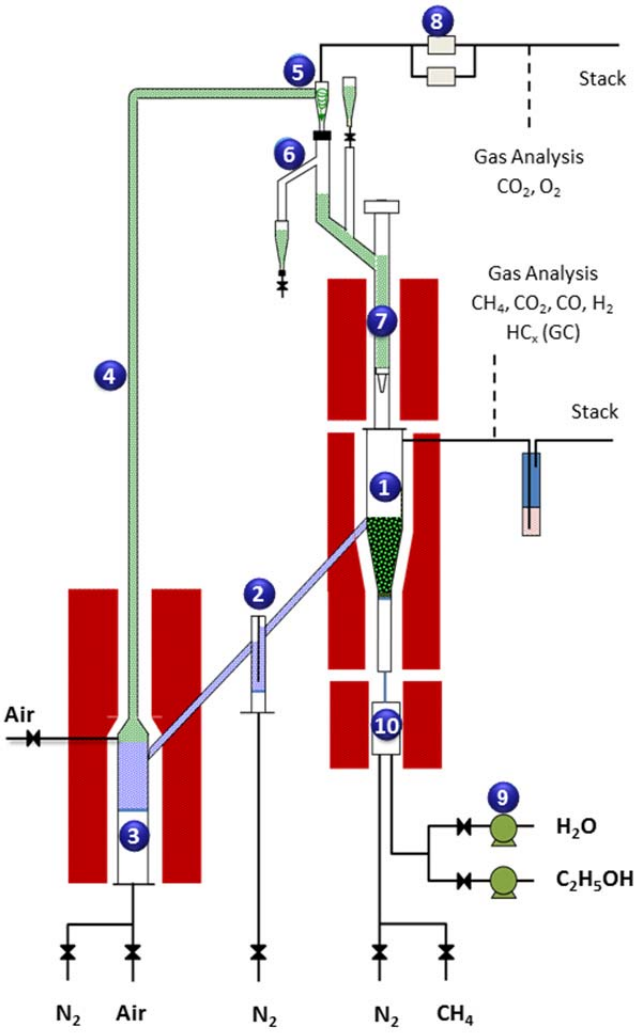

Fig. 2. Schematic diagram of the 1 kW_{th} chemical-looping reforming unit (ICB-CSIC-liq1).

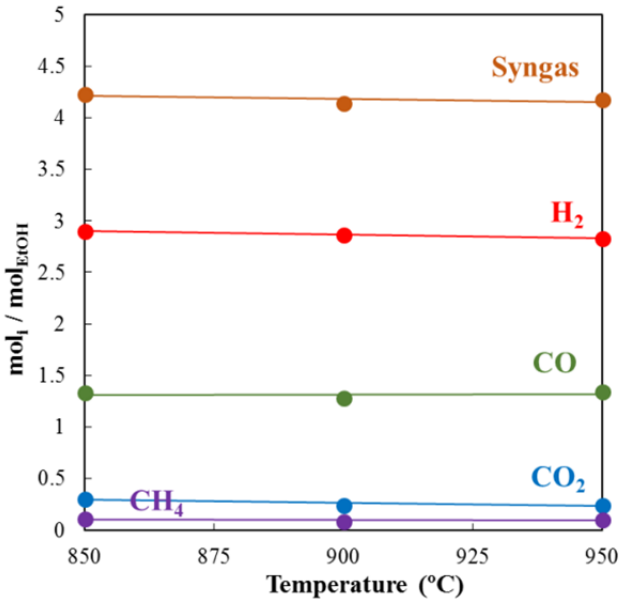

Fig. 3. Effect of the fuel reactor temperature on the syngas composition. OC= NiO21-γAl_2O_3, H_2O/EtOH=1, O_{NiO}/EtOH=1.2.

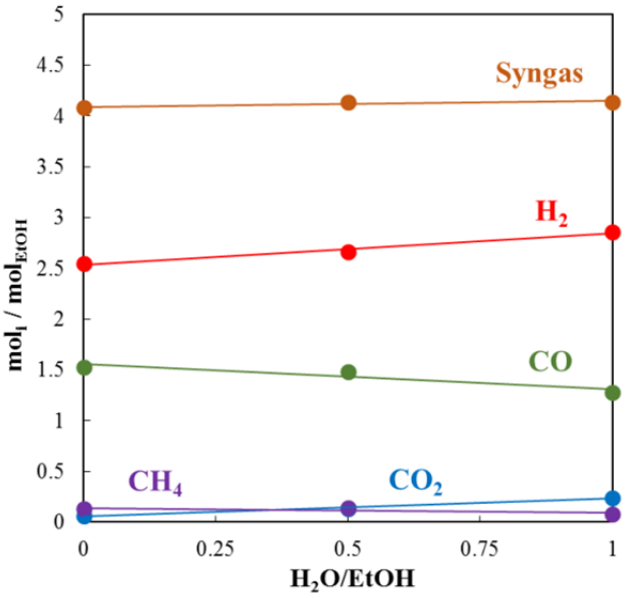

Fig. 4. Effect of the H_2O/EtOH molar ratio in the syngas composition. OC=NiO21-γAl_2O_3, T_{FR}= 900 ºC, O_{NiO}/EtOH=1.2.

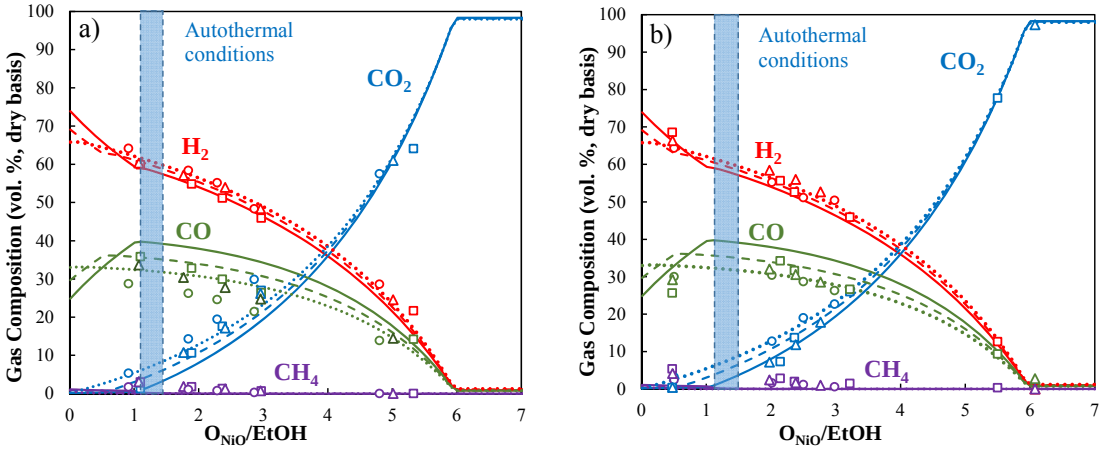

Fig. 5. Syngas composition obtained as a function of the oxygen-to-fuel molar ratio. a) NiO21-γAl_2O_3 , b) NiO18-αAl_2O_3. T= 900 ºC. Lines represent thermodynamic equilibrium. (□,___, H_2O/EtOH = 0), (△,- - -, H_2O/EtOH = 0.5), (○,…., H_2O/EtOH = 1).

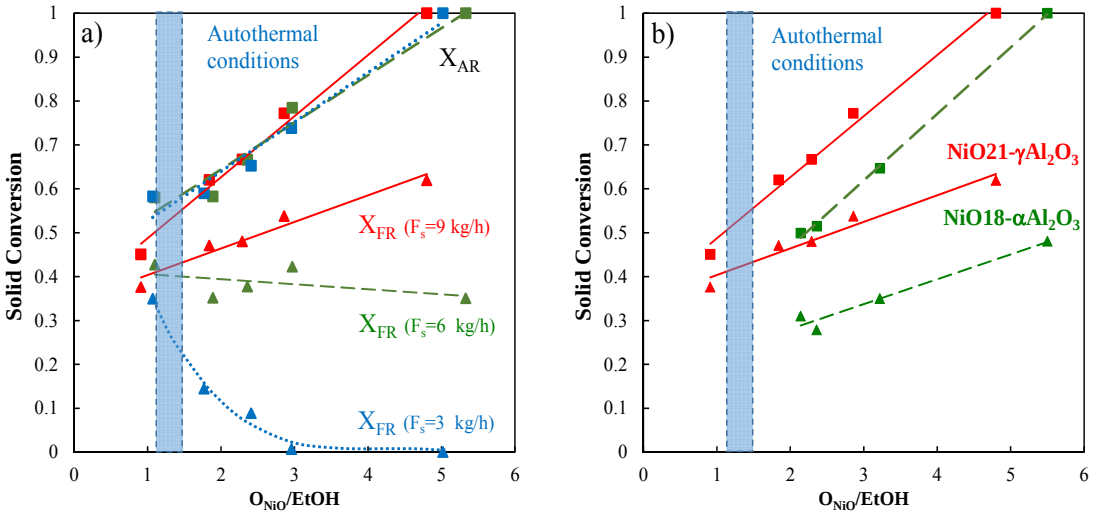

Fig. 6. Solid conversion at the exit of the fuel and air reactors for different solid circulation rates. a) OC= NiO21-γAl_2O_3, b) NiO21-γAl_2O_3 and NiO18-αAl_2O_3 with F_s=9 kg/h. T_{FR}= 900 ºC. (□, Solid conversion in the AR), (△, Solid conversion in the FR).